10.24425/acs.2020.132585

Archives of Control Sciences
Volume 30(LXVI), 2020
No. 1, *pages 47–76*

The combined effect of fractional filter and Smith Predictor for enhanced closed-loop performance of integer order time-delay systems: some investigations

SHAIVAL HEMANT NAGARSHETH and SHAMBHU NATH SHARMA

This paper proposes a generalized fractional controller for integer order systems with time delay. The fractional controller structure is so adopted to have a combined effect of fractional filter and Smith predictor. Interestingly, the resulting novel controller can be decomposed into fractional filter cascaded with an integer order PID controller. The method is applied to two practical examples i.e. liquid level system and Shell control fractionator system. The closed-loop responses resulting from the proposed method are compared with that of the available methods in the literature. For quantitative evaluations of the proposed method, Integral Absolute Error (IAE) and Integral Square Control Input (ISCI) performance criteria are employed. The proposed method effectively enhances the closed-loop response by improving the IAE values, reducing the control effort inputs to achieve the desired output. The disturbance rejection and robustness tests are also carried out. The robustness test reveals a significant improvement in the maximum absolute sensitivity measure. That is displayed in numerical simulations of the paper.

Key words: generalized fractional controller, Smith predictor, time delay system, generalized inverse, Bode's ideal transfer function

1. Introduction

Systems with time delay are ubiquitous in industry. As a result, the controller design becomes more complicated due to the presence of time delays in the system. The controller action can execute and affect the controlled variable only after the dead time fades away. Due to the presence of dead-time, there is a limiting value to the proportional gain of the controller ([24], p. 603). For the larger dead-time case, the limit to adjust the controller gain will be smaller.

S.H. Nagarsheth, the corresponding author (E-mail: shn411@gmail.com) and S.N. Sharma (E-mail: snsvolterra@gmail.com) are with Department of Electrical Engineering, Sardar Vallabhbhai National Institute of Technology, Surat 395007, Gujarat, India.

Received 28.03.2019. Revised 26.01.2020.

Thus, if the user tries to achieve a faster response by increasing the controller gain, it will lead to oscillations in the output. Further, if the controller gain is increased beyond the allowable limit, it leads to instability in the closed-loop system ([35], p. 214). This can be considered as poor control, which will have devastating consequences. For example, oscillations in the output will have an influence on the performance of industrial combustion systems and industrial reactors [19]. That causes pressure pulsations with high amplitudes, which lead to ill-consequences, e.g. violent vibrations damaging the system [15]. To deal with delay dominant systems, dead time compensator [34] and analytical predictor [22] were designed. The compensator removes the pernicious effect of the time delay element in the controlled output. Wong and Seborg [39] explored the relation between Smith predictor and analytic predictor.

PID controllers are the most commonly used control algorithms in process control techniques due to their ubiquitous behaviour and realization property. Tuning of PID parameters in time as well as frequency domain can be found in Åström and Hägglund [3]. The ubiquity of PID controllers is not just limited to the integer order but goes further to fractional order. Podlubny [28] pioneered the concept of Fractional-order PID (FOPID) controllers. The main contribution towards the world of fractional controllers can be traced back to the work of H.W. Bode. That is popularly known as Bode's ideal transfer function [8]. Importantly, the Bode's ideal transfer function in the closed-loop setting becomes the fractional filter transfer function of the equivalent embedded internal model [5]. Fractional PID controller for reduced order models is carried out by Yumuk et al. [40]. However, in their work Smith predictor is not accounted for. Bettayeb et al. [6] designed an IMC based fractional filter-PID controller without the Smith predictor. Auto-tuning of fractional order controllers for several industrial applications can be found in Monje et al. [21]. A good exposition regarding the comparison between the two degree of freedom (2DOF) integer order PID controller and 2DOF fractional order PID is cited in Bingi et al. [7]. The difficulty posed by the time delay element increases more with multi-input, multi-output (MIMO) systems, where different time delays are present in loops with their interaction. In the Laplace domain, the MIMO systems are represented by the transfer function matrix that is square or non-square depending on the number of inputs and outputs. The measure of these interactions for the non-square MIMO system was presented by Reeves and Arkun [32]. The concept of dead time compensator was extended to MIMO processes by Alevisakis and Seborg [1]. For the multi-loop system, it is important to decide the controller pairing based on which the decentralized control can be realized on the system. The controllers pairing is adjudged using RGA (Relative Gain Array) techniques [9]. Rao and Chidambaram [30] designed a Smith predictor for a non-square MIMO fractionator system with multiple time delays. Chen et al. [11] designed a new control method for the MIMO FOPDT non-square systems, see

Wang et al. [37, 38] as well for a good source of auto-tuned multivariable PID controllers.

The prime intent of this paper is to investigate and reveal the combined effect of the Smith predictor and the fractional filter with the idea of achieving better-controlled output response in the sense of overshoot, robustness, disturbance rejection, less IAE, and ISCI values. The uniqueness of the proposed fractional controller structure lies with the addition of the Smith predictor into the inner feedback loop. The feedback setup is such that the derivation of the fractional filter structure of n-th order time delay system accounts for the contribution from the Smith predictor. Notably, the proposed fractional controller can be interpreted as a series combination of the fractional filter and industrial controller, e.g. PID controller. That is the result of adopting the IMC design methodology by replacing the filter used in conventional IMC with the Bode's ideal transfer function and encompassing the Smith predictor in the inner feedback loop. The theoretical development of this paper is applied to two appealing practical examples. First, to test the effectiveness of the proposed method, investigations are carried on a single-input, single-output liquid level system. Then, the investigations are also carried out for a non-square MIMO Shell control fractionator problem. In order to unfold insights into the Smith predictor and the fractional filter, the control configuration of Stephanopoulos ([35], p. 386) is considered for investigations. The stability of the proposed controller is examined via the notion of the fractional characteristic polynomial for the fractionator control problem. The efficacy of the controller of this paper is tested quantitatively by the improved measure of the Integral Absolute Error (IAE) and the Integral Square Control Input (ISCI) performance indices. The robustness of the proposed controller is adjudged through the measure of the maximum absolute sensitivity which reveals the greater stability margin of the proposed controller.

2. Mathematical preliminaries

This section consists of mathematical preliminaries that are useful for carrying out theoretical development and application of the proposed controller to the appealing system.

2.1. Bode's ideal transfer function

The fractional filter used in this study is the 'Bode's ideal transfer function' [5, 8], suggested by Bode. The open loop form is

$$F(s) = \frac{1}{\tau_c s^{\gamma+1}}, \qquad \gamma \in R,$$

where $\tau_c = 1/\omega_c^{\gamma+1}$, except γ takes non-negative integers.

The closed-loop transfer function with unity feedback becomes $\dfrac{1}{1+\tau_c s^{\gamma+1}}$. The magnitude and phase properties of the fractional filter are direct consequences of the Bode's ideal transfer function coupled with unity feedback, see Fig. 1. The use of τ_c and γ is discussed in Section 3.

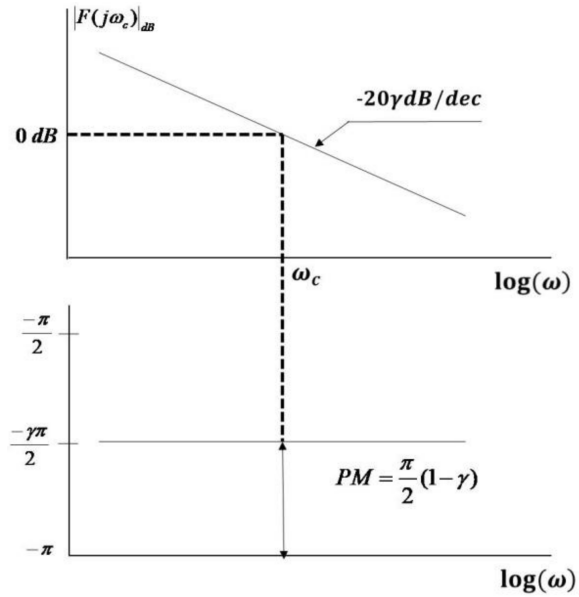

Figure 1: Bode diagrams of amplitude and phase of $F(s)$

2.2. Gain arrays

The RGA, suggested by Bristol [9], is a methodical approach to measure the interactions amongst the inputs and outputs of a multi-loop process control problem. This systematic approach requires only the steady state gain matrix and provides the measure of the interactions as well as the recommendation concerning the most effective controller pairing [33]. Suppose $Y(s)$ is an $m \times 1$ output vector and $U(s)$ is an $n \times 1$ input vector of the multivariable process. Now, $G(s)$ is the transfer matrix, where, $G_{ij} = \dfrac{k_{ij}\, e^{-t_{dij}s}}{1+\tau_{ij}s}$ with $k_{ij}, t_{dij}, \tau_{ij}$ are the steady-state gain, dead time and time constant respectively of the i-th output with respect to j-th input. Using the generalized inverse result of Graybill et al. [14], the non-square RGA [10] becomes

$$\lambda^N = G \circ (G^+)^T, \tag{1}$$

where the notation '$\circ$' denotes the Schur product, i.e. element-wise product of matrices. The matrix G^+ is a generalized inverse, the entries of the steady state

gain matrix G are obtained by evaluating it at $s = 0$. Alternatively, the non-square RGA matrix (1) can also be stated in the component-wise setting as

$$\lambda_{ij}^{N} = G_{ij} G_{ji}^{+} .$$

Based on the above formula, the effective controller pairing [33] between the respective output and input can be recommended if $\lambda_{ij}^{R} \geqslant 0.5$.

The RNGA [16] has proven a useful alternative to the RGA. The Relative Normalized Gain Array (RNGA) includes the dynamics of the system as well [16]. The Normalized Gain Array (NGA) can be formulated as $N = K \circ \widetilde{\tau}_{ar}$, where $\widetilde{\tau}_{ar} = (\widetilde{\tau}_{ar})_{ij} = (\tau_{ar})_{ij}^{-1}$, K is the steady state gain matrix and τ_{ar} is average residence time matrix. The average residence time for the transfer function G_{ij} associated with the i-th output and j-th input is the summation of the time constant τ_{ij} and the dead time t_{dij}, i.e. $(\tau_{ar})_{ij} = \tau_{ij} + t_{dij}$. Now, the Relative Normalized Gain Array (RNGA) is defined as

$$\lambda^{RN} = N \circ (N^{+})^{T}. \tag{2}$$

2.3. A Generalized Internal Model Control

Morari et al. [23], Rivera et al. [31] and Garcia et al. [12] developed a comprehensive model-based controller design method, i.e. Internal Model Control (IMC). This method is based on assumed process models which lead to an inquisitive expression for the controller setting. The generalized feedback and its equivalent IMC block diagrams are shown in Fig. 2 and Fig. 3. The model response $\widetilde{Y}_p$ is calculated by the control signal H and the internal process model $\widetilde{G}_p$.

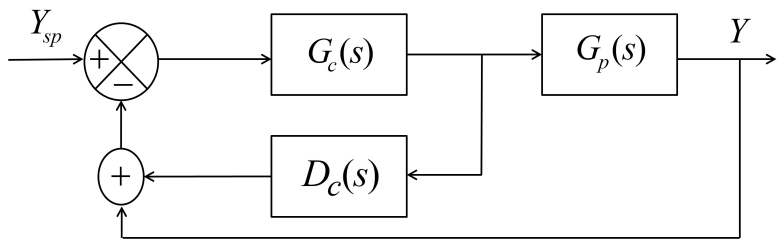

Figure 2: Classical feedback loop with Smith predictor

The embedded model response is subtracted from the actual response Y and the difference will become an input signal to the IMC controller G_{IMC}.

$$G_c'(s) = \frac{G_{IMC}(s)}{1 - G_{IMC}(s)\,\widetilde{G}_p(s)},$$

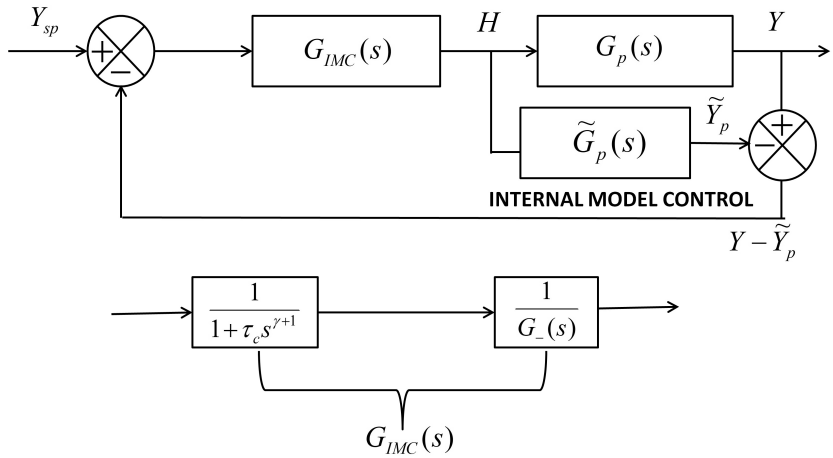

Figure 3: Generalized IMC based feedback loop

where $G_{IMC}(s) = \dfrac{1}{\widetilde{G}_-(s)} F(s)$, see Fig. 3. The IMC controller $G_{IMC}(s)$ consists of a filter $F_c(s) = \dfrac{1}{1+\tau_c s^{\gamma+1}}$ and the reciprocal of$\widetilde{G}_-(s)$. The term $\widetilde{G}_-(s)$ contains the non-singular part of the plant transfer function.

Greater detail about the IMC method can be found in Seborg et al. [33]. The generalized IMC of the paper is attributed to the following two embeddings, i.e. (i) Smith predictor coupled controller (ii) fractional filter coupled with reciprocal of the minimum phase part of the plant transfer function in the lieu of integer.

3. Theoretical development

A refined structure of the controller transfer function of control literature is uniquely developed to combine the benefits of the fractional filter and Smith predictor. This is achieved by designing a fractional controller comprising a fractional filter coupled with the integer-order controller and the Smith predictor. Here, we sketch the main controller transfer function result of the linear feedback system that accounts for the Smith predictor, fractional filter and the plant transfer function.

Theorem 1 *Suppose the plant transfer function $G_p(s)$ that embeds the properties of the underlying dynamics of the plant. Consider the predictor transfer function $D_c(s) = \dfrac{1-e^{-t_d s}}{e^{-t_d s}} G_p(s)$. Then, the generalized fractional controller transfer*

function is

$$G_c(s) = \frac{e^{-t_d s}\widetilde{G}_+(s)}{\widetilde{G}_p(s)\left((1+\tau_c s^{\gamma+1})e^{-t_d s} - \widetilde{G}_+(s)\right)},$$

where $G_p(s) = \widetilde{G}_-(s)\,\widetilde{G}_+(s)$.

Proof. Here, we sketch the proof of the Theorem using the notion of equivalence of two systems. The idea is to replace a closed-loop system with another closed-loop system embedded with the auxiliary plant. Note that Fig. 2 is equivalent to Fig. 3. On solving the inner loop, embedding the Smith predictor $D_c(s)$ and $G_c(s)$, the control block of Fig. 2 reduces to

$$G_c'(s) = \frac{G_c(s)}{1 + D_c(s)\,G_c(s)}. \tag{3}$$

According to the IMC design procedure, Fig. 3

$$G_c'(s) = \frac{G_{IMC}(s)}{1 - G_{IMC}(s)\,\widetilde{G}_p(s)}. \tag{4}$$

The IMC controller $G_c'(s)$ is an immediate consequence of the algebra of the closed-loop system of Fig. 2 and its equivalence to Fig. 3. After combining (3), (4) and utilizing the predictor transfer function $D_c(s) = \dfrac{1-e^{-t_d s}}{e^{-t_d s}}\,G_p(s)$ [35], we arrive at the controller transfer function

$$G_c(s) = \frac{1}{\dfrac{\widetilde{G}_-(s)}{F_c(s)} - \widetilde{G}_p(s) - \dfrac{(1-e^{-t_d s})}{e^{-t_d s}}\,G_p(s)}. \tag{5}$$

Note that the embedded transfer function, i.e. the internal model transfer function, can be regarded as $\widetilde{G}_p(s) = \widetilde{G}_-(s)\,\widetilde{G}_+(s)$, where $\widetilde{G}_-(s)$ has the minimum phase property. Consider the fractional filter transfer function $F_c(s) = \dfrac{1}{1+\tau_c s^{\gamma+1}}$. After embedding the internal model transfer function $\widetilde{G}_p(s)$, Eq. (5) can be further recast as

$$\begin{aligned} G_c(s) &= \frac{1}{\dfrac{(1+s^{\gamma+1}\tau_c)\widetilde{G}_p(s)}{\widetilde{G}_+(s)} - \widetilde{G}_p(s) - \dfrac{(1-e^{-t_d s})}{e^{-t_d s}}G_p(s)} \\ &= \frac{e^{-t_d s}\widetilde{G}_+(s)}{e^{-t_d s}(1+s^{\gamma+1}\tau_c)\widetilde{G}_p(s) - e^{-t_d s}\widetilde{G}_p(s)\,\widetilde{G}_+(s) - (1-e^{-t_d s})\widetilde{G}_+(s)G_p(s)}. \end{aligned}$$

Thus, a convenient form of the controller transfer function is

$$G_c(s) = \frac{e^{-t_d s}\widetilde{G}_+(s)}{\widetilde{G}_p(s)\left((1+\tau_c s^{\gamma+1})e^{-t_d s} - \widetilde{G}_+(s)\right)}. \tag{6}$$

The structure of the controller $G_c(s)$ is general and holds for n-th order stable integer time-delay systems. □

Here, we illustrate two appealing practically useful cases. That demonstrates the decomposition of the generalized fractional controller of the Theorem of the paper into fractional filter and integer order controller. The fractional controller transfer functions for a general class of higher-order time-delay systems are in Appendix A, see Table A.

Case 1. Consider the first-order plus dead time (FOPDT) transfer function

$$G_p(s) = \frac{k e^{-t_d s}}{\tau s + 1}. \tag{7}$$

We wish to achieve the controller transfer function that accounts for the controller fractionality and Smith predictor correction term. The controller fractionality is attributed to the filter of the IMC controller. After considering the Pade-approximate exponential term, we have

$$e^{-t_d s} \approx \frac{1 - \frac{t_d s}{2}}{1 + \frac{t_d s}{2}}, \qquad \widetilde{G}_p(s) = G_p(s) = \frac{k e^{-t_d s}}{\tau s + 1} \approx \frac{k\left(1 - \frac{t_d s}{2}\right)}{(\tau s + 1)\left(1 + \frac{t_d s}{2}\right)}. \tag{8}$$

Note that

$$\widetilde{G}_+(s) = \widetilde{G}_p(s)\,\widetilde{G}_-^{-1}(s) = \left(1 - \frac{t_d s}{2}\right), \tag{9}$$

where $\widetilde{G}_-^{-1}(s)$ is the inverse of the non-minimum phase part of the embedded plant transfer function. After combining (7)–(9) with (6) and simplifying them, we arrive at the generalized fractional filter-PID controller transfer function, i.e.

$$\begin{aligned} G_c(s) &= \frac{(\tau s + 1)\left(1 + \frac{t_d s}{2}\right)}{k\tau_c s^{\gamma+1} + k\left(1 - \frac{t_d s}{2}\right) - k\left(1 + \frac{t_d s}{2}\right)} \\ &= \frac{1}{\tau_c s^{\gamma} - t_d}\left(\frac{\tau + \frac{t_d}{2}}{k} + \frac{1}{k\,s} + \frac{\tau t_d}{2k}s\right). \end{aligned} \tag{10}$$

After considering the generalized controller transfer function of (10) for a FOPDT system in Fig. 2, we get Fig. 4.

The generalized fractional order controller transfer function of Fig. 4 has two parts. The first part is the fractional part, which is in series with the second part. The second part is an integer PID, see Fig. 4. Here, we explain the contribution of the Smith predictor by introducing the notion of fractional characteristic and fractional quasi-characteristic polynomials. Fig. 4 displays a specific case of the proposed method by considering the FOPDT system with the Smith predictor. An alternative version of Fig. 4(a) is illustrated in Fig. 4(b). Both the Figs. 4(a) and 4(b) describe the equivalent systems. The equivalent feedback loop in Fig. 4(b) shows that the controller works on the signal coming from a system without dead-time after embedding the Smith predictor.

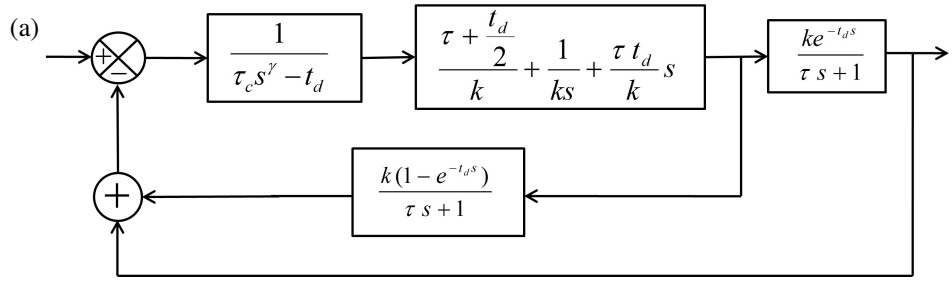

Proposed feedback loop embedding Smith predictor

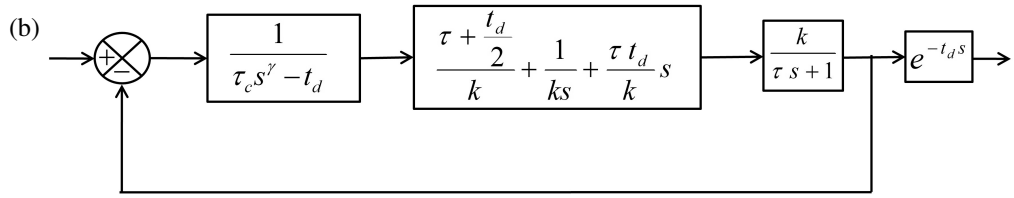

Equivalent feedback loop embedding Smith predictor

Figure 4: Feedback loop with Smith predictor and fractional filter

As a result of this, the overall closed-loop transfer function 'embedding' the Smith predictor term becomes

$$\frac{Y(s)}{Y_{sp}(s)} = \left(\frac{G_c(s)\, G_p^*(s)}{1 + G_c(s) G_p^*(s)} \right) e^{-t_d s}. \tag{11}$$

where the terms $Y(s)$ and $Y_{sp}(s)$ denote the Laplace transforms of the output and the setpoint respectively. The term $G_c(s)$ denotes the controller transfer function

and $G_p^*(s)$ is the plant transfer function without dead-time. After embedding

$$G_P^*(s) = \frac{k}{\tau s + 1},$$

$$G_c(s) = \frac{1}{\tau_c s^\gamma - t_d}\left(\frac{\tau + \frac{t_d}{2}}{k} + \frac{1}{ks} + \frac{\tau t_d}{2k}s\right),$$

in (11), Eq. (11) reduces to

$$\frac{Y(s)}{Y_{sp}(s)} = \frac{\left(1 + \frac{t_d}{2}s\right)e^{-t_d s}}{s\left(\tau_c s^\gamma - \frac{t_d}{2}\right) + 1}. \tag{12}$$

After 'ignoring' the Smith predictor correction term in *Case 1*, the generalized fractional order controller transfer function of (6) reduces to

$$G_c(s) = \frac{\widetilde{G}_+(s)}{(1 + s^{\gamma+1}\tau_c)\,\widetilde{G}_p(s) - \widetilde{G}_p(s)} = \frac{1}{\tau_c s^\gamma}\left(\frac{\tau + \frac{t_d}{2}}{k} + \frac{1}{ks} + \frac{\tau t_d}{2k}s\right).$$

The overall closed-loop transfer function, *without* the Smith predictor, is given by

$$\frac{Y(s)}{Y_{sp}(s)} = \frac{G_c(s)\,G_p^*(s)\,e^{-t_d s}}{1 + G_c(s)\,G_p^*(s)e^{-t_d s}}. \tag{13}$$

Consider $G_P^*(s) = \dfrac{k}{\tau s + 1}$ and $G_c(s) = \dfrac{1}{\tau_c s^\gamma}\left(\dfrac{\tau + \frac{t_d}{2}}{k} + \dfrac{1}{k\,s} + \dfrac{\tau\,t_d}{2k}s\right)$, Eq. (13) reduces to a specific case, i.e.

$$\frac{Y(s)}{Y_{sp}(s)} = \frac{\left(1 + \frac{t_d}{2}s\right)e^{-t_d s}}{\tau_c s^{\gamma+1} + \left(1 + \frac{t_d}{2}s\right)e^{-t_d s}}. \tag{14}$$

Eq. (14) tells that the denominator polynomial becomes a fractional-quasi characteristic polynomial in the absence of the Smith predictor. After careful observation of (14) and (12), the absence of the dead-time in (12) is clear. This leads to a fractional characteristic polynomial in the lieu of the fractional-quasi polynomial. This demonstrates the usefulness of the Smith predictor in the sense

that the time delay term from the denominator polynomial of the transfer function of the proposed closed-loop scheme vanishes. As a result of this, the controller of the equivalent closed-loop will work with a feedback signal from a system that no longer contains a time delay term, see Fig. 4(b). This effectively removes the pernicious effect of the time delay term. Notably, for the fractional parameter $\gamma = 0$, we arrive at the IMC based integer PID controller transfer function [33], i.e.

$$G(s) = \frac{\tau + \frac{t_d}{2}}{k\tau_c} + \frac{1}{k\tau_c s} + \frac{\tau t_d}{2k\tau_c}.$$

□

Case 2. Consider a Second Order Plus Dead Time (SOPDT) transfer function

$$G_p(s) = \frac{ke^{-t_d s}}{(\tau_1 s + 1)(\tau_2 s + 1)}. \tag{15}$$

After considering the Pade-approximate exponential term, we have

$$\begin{aligned} \widetilde{G}_p(s) = G_p(s) &= \frac{ke^{-t_d s}}{(\tau_1 s + 1)(\tau_2 s + 1)} \\ &\approx \frac{k\left(1 - \frac{t_d s}{2}\right)}{(\tau_1 s + 1)(\tau_2 s + 1)\left(1 + \frac{t_d s}{2}\right)}, \end{aligned} \tag{16}$$

where $\widetilde{G}_p(s) = \widetilde{G}_+(s)\,\widetilde{G}_-(s)$, with $\widetilde{G}_-(s) = \dfrac{k}{(\tau_1 s + 1)(\tau_2 s + 1)\left(1 + \frac{t_d s}{2}\right)}$.

On combining (16) with developed (6) of the theorem, the generalized fractional order controller transfer function becomes

$$\begin{aligned} G_c(s) &= \frac{(\tau_1 s + 1)(\tau_2 s + 1)\left(1 + \frac{t_d s}{2}\right)}{\left(k\tau_c s^{\gamma+1} - k\frac{t_d s}{2}\right)} \\ &= \frac{\left(1 + \frac{t_d s}{2}\right)}{\left(\tau_c s^{\gamma} - \frac{t_d}{2}\right)}\left(\frac{\tau_1 + \tau_2}{k} + \frac{1}{k\,s} + \frac{\tau_1\,\tau_2}{k}s\right). \end{aligned}$$

Remark 1 *The fractional filter parameter τ_c and the fractionality γ, are adjudged using the notion of the ideal Bode's transfer function in open and closed-loop settings. The ideal Bode transfer function in the closed-loop setting becomes the*

fractional filter transfer function [5]. Calculations suggest that the phase margin of the fractional filter is approximately equal to the linear feedback system of Fig. 2. As a result of this, we have

$$\gamma = \frac{\pi - PM}{\pi/2} - 1, \qquad \tau_c = \frac{1}{\omega_c^{\gamma+1}}. \tag{17}$$

The benefit of embedding the fractional filter into the IMC method stems from the fact that the overshoot has a relationship with the fractionality of the filter ([5], p. 311). Greater detail on the formal proof of arriving at the relationship between the filter fractionality and the overshoot can be found in Barbosa et al. ([5], p. 311). The Bode's ideal loop transfer function becomes the closed-loop reference model. The filter parameters τ_c and γ are adequately chosen by the designer [2]. A note on the practical implementation of the fractional filter is discussed in Appendix B of the paper.

4. Appealing examples

In order to evaluate the efficacy of the generalized fractional controller of the paper, the proposed controller is effectuated to two appealing practical examples, i.e. (i) liquid level system (ii) Shell control fractionator problem. The simulation is carried out for the step setpoint change in the desired value of the output and for disturbance rejection case as well. The performance of the closed-loop response for both the examples is evaluated based on improvements in the Integral Absolute Error (IAE), Integral of Square Control Index (ISCI) values and sensitivity performance indices to test the robustness of the proposed method.

4.1. SISO example

As a first example, a liquid level system which consists of a low pressure flowing water circuit is considered [6, 21]. This practical example is described by the transfer function $G_p(s)$ as

$$G_p(s) = \frac{3.13e^{-50s}}{433.3s + 1}. \tag{18}$$

The controller tuning method proposed in the Theorem of this paper is used to design the controller for the transfer function in (18). The resulting controller transfer function $G_c(s)$ is

$$G_c(s) = \frac{1}{136.22s^{0.111} - 25}\left(146.43 + \frac{0.3194}{s} + 3461.1s\right). \tag{19}$$

The PID parameters of the controller transfer functions $G_c(s)$ are achieved using (18) and (10) of the paper. Here, the PID parameters are directly expressed as a function of system parameters to make the tuning a tribulation-free, i.e. the IMC method.

We observe the effect of variations in the two filter parameters γ and τ_c. It is worth to mention that fractionality of the filter also contributes to reducing oscillations in the overshoot sense. For the desired overshoot of the setpoint response, the value of fractionality γ can be reckoned. After using the "cftool" function of MATLAB [18] for our system parameters, we arrive at a second-order polynomial relation between the fractionality γ and the overshoot M_p, i.e.

$$M_p \approx 2.921\gamma^2 - 0.6814\gamma + 0.08602. \tag{20}$$

The above relation in (20) reveals that the increase in the fractionality of the filter contributes to the increase in the overshoot of the closed-loop system. A graphical representation of the above relation between the overshoot M_p and the fractionality γ is displayed in Fig. 5.

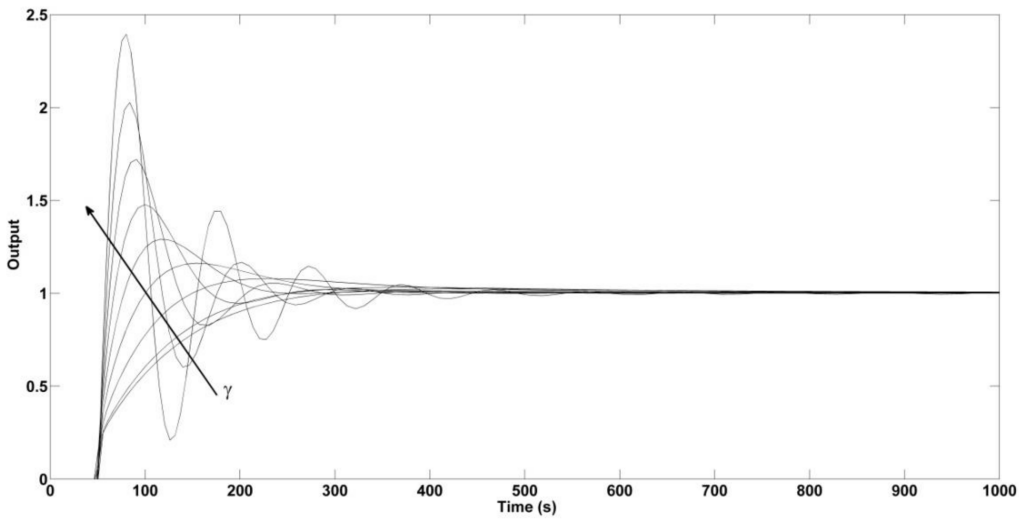

Figure 5: Step response with variations in γ

Fig. 5 shows an increase in the overshoot of the closed-loop response with an increase in γ. Another revelation is that an increase in the filter parameter τ_c leads to the sluggish response of the closed-loop, see Fig. 6. The filter parameter τ_c and the fractionality γ are adjudged using the notion of the Bode's ideal transfer function approach. This is described in Remark of the paper. Here the filter parameters $\tau_c = 136.22$ and $\gamma = 0.111$ corresponds to the overshoot $M_p \approx 0.04$.

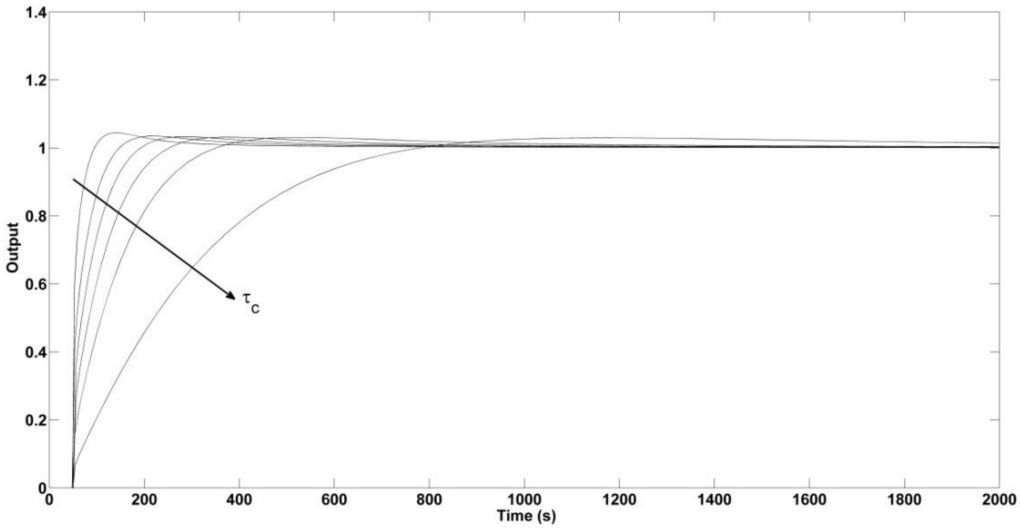

Figure 6: Step response with variation in τ_c

4.1.1. Stability assessment

The stability analysis of the proposed fractional closed-loop system hinges on the Riemann surface ([17], p. 200). It is important to note that the stability of the proposed fractional filter embedded closed-loop system can be rephrased using the notion of the fractional characteristic polynomial. Here, we explain briefly the stability of the fractional characteristic polynomial using 'the change of variables' and the graphical assessment is displayed using the FOMCON toolbox of Matlab [20]. The structure of the fractional characteristic polynomial associated with the proposed closed-loop setup is

$$f(s) = \tau_c s^{\gamma+1} - \frac{t_d}{2}s + 1. \tag{21}$$

The structure changes for the specific tuning parameters. The specific structure of the fractional characteristic polynomial associated with the closed-loop of SISO example is

$$f(s) = 136.22s^{1.111} - 25s + 1.$$

The roots of the fractional characteristic polynomials are located in the s plane, where $s = \sigma + j\omega$. The calculation of roots of the fractional polynomial becomes quite intractable, thus, we introduce the mapping of the s plane to a plane associated with the equivalent characteristic polynomial. Choose $\lambda = s^{\beta}$, we arrive at the characteristic polynomial. The associated characteristic polynomial is

$$f\left(\lambda^{1/\beta}\right) = \widetilde{f}(\lambda) = 136.22\lambda^{1111} - 25\lambda^{1000} + 1,$$

where $s^{0.001} = \lambda$. For the stability of the proposed fractional closed-loop system, the absolute values of the angles of roots of the associated characteristic polynomials are larger than $\frac{\beta\pi}{2}$, i.e. $|\angle\lambda_i| > \frac{\beta\pi}{2}$, the system is said to be stable ([20], p. 237). The graphical analysis in Fig. 7 confirms the stability of the fractional system of the paper, i.e. the condition $|\angle\lambda_i| > \frac{\beta\pi}{2}$ holds for the associated characteristic polynomial. Fig. 7 displays the stability assessment for closed-loop system associated with the liquid level system.

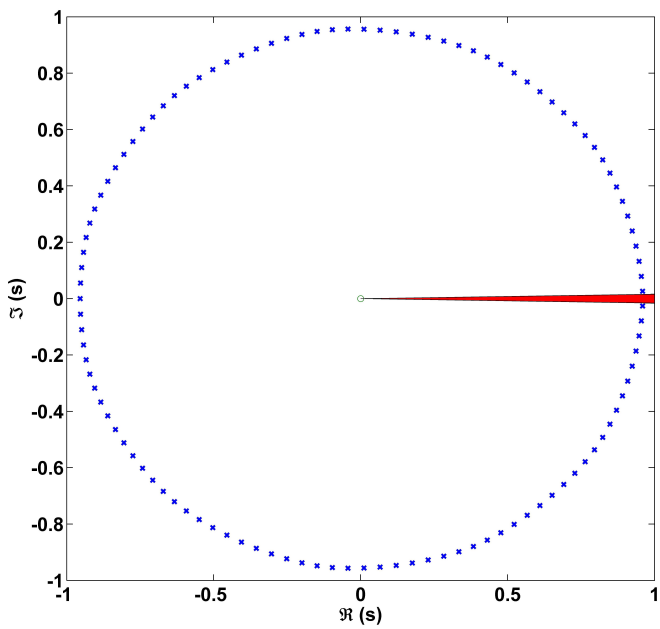

Figure 7: Stability assessment for closed-loop liquid level system

It is observed from Fig. 7 that no angles of roots of the associated characteristic polynomial for the closed-loop lie inside the principal sheet of the Riemann surface. That is suggestive of the stable closed-loop system. In addition to the stability, we investigate the following: (i) reference tracking using the IAE and ISCI indices (ii) disturbance rejection response (iii) robustness test.

4.1.2. Reference tracking response

The step response simulation is carried out to evaluate the superiority and usefulness of the proposed method. The resulting closed-loop step response of the proposed method is compared with that of the closed-loop response resulting from the controller design of Bettayeb and Mansouri [6] and Monje et al. [21]. Fig. 8(a) displays the closed-loop response for a unit step setpoint change of three

methods. It is clear from Fig. 8(a) that closed-loop response associated with the proposed method of this paper has a faster response with less overshoot than that of the other two methods. Fig. 8(b) shows the control law comparison of all the three methods. A zoomed image of the control law associated with the proposed method is shown in Fig. 8(c). Fig. 8(b) reveals that the control law of Monje et al. [21] achieves a maximum value greater than 20, which is more than that of the other two methods. From Fig. 8(c) one can observe the advantage of the method proposed in this paper since the control law of the proposed closed-loop achieves a value of 0.009 only. That is relatively less than the other methods of the literature. To judge the ability of the linear feedback system, the Integral Square Control Input (ISCI) is employed, i.e. $ISCI = \int_{o}^{t} u^2(\tau)\,\mathrm{d}\tau$. The less value of the ISCI is indicative of the less effort required from the controller to achieve the desired output ([27], p. 535).

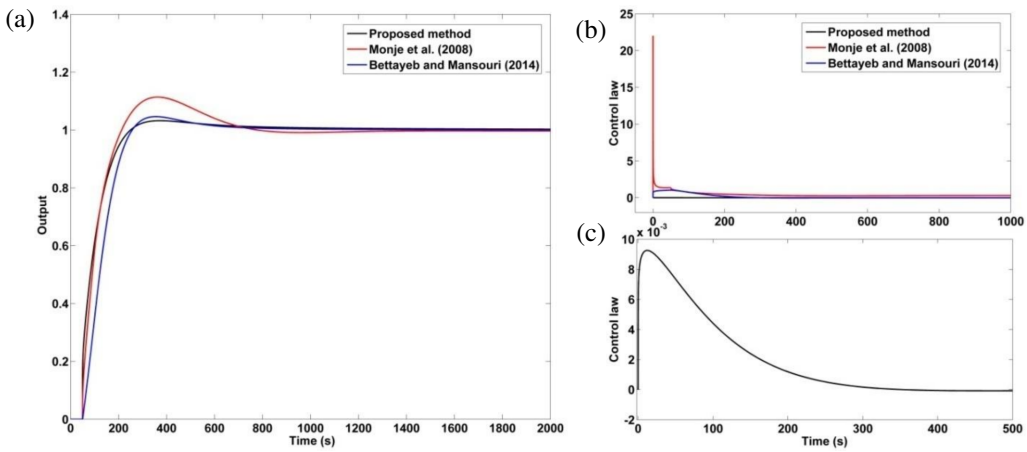

Figure 8: Closed-loop step response of the liquid level system for a unit step setpoint change

Table 1 shows comparative closed-loop performance indices for all three methods. The IAE value associated with the closed-loop of the paper is the least,

Table 1: Performance indices of the liquid level system

Method	The IAE for liquid level system	Control effort in the inputs (ISCI)
Proposed method	66.27	344.5
Monje et al. (2008)	194.9	402.7
Bettayeb and Mansouri (2014)	143.8	351.2

indicating better performance of the proposed fractional controller. The values in Table 1 reveal the advantage, usefulness and superior performance of the proposed method.

4.1.3. Disturbance rejection response

To achieve the superiority of the controller under a variety of conditions, we consider a disturbance transfer function [6] $G_d(s) = 1/(100s + 1)$ to study the effectiveness of three methods for disturbance rejection scenario. Fig. 9(a) shows the response when the disturbance $G_d(s)$ with a step input of magnitude 0.1 is acting on the controlled output. Whereas, Fig. 9(b) displays the efforts put by all the three controllers to reject the given disturbance. The black line in Fig. 9(a) denotes the disturbance rejection response associated with the fractional controller of the paper. The disturbance response of the proposed method has the least overshoot in comparison to the other available controllers in the literature. The red line in Fig. 9(a) represents the disturbance rejection for Monje et al. [21] closed-loop. Bettayeb and Mansouri [6] disturbance rejection graph is denoted by blue line.

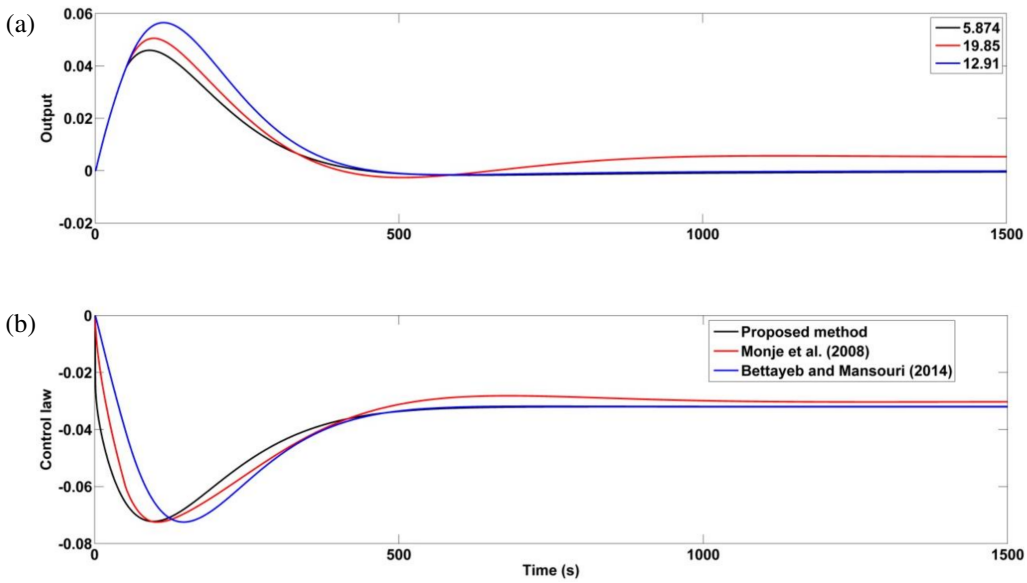

Figure 9: Disturbance rejection response for liquid level system

IAE values for all the three methods are noted in Fig. 9(a). The IAE value associated with the proposed method is 5.874, see Fig. 9(a) That is relatively less than the other methods, which is indicative of the better response generating from the proposed fractional controller of the paper.

4.1.4. Robustness test

The qualitative characteristics of the linear feedback system vary with process parameter variations and input disturbances [4]. The sensitivity analysis is an efficient tool to measure the robustness of a system under process parameter variations and input disturbances. The variation in the process parameters affects the stability margin as well as the robustness ([4], p. 323). Here, we explain the robustness test of the fractional control of the paper by introducing the notion of the sensitivity function, maximum absolute sensitivity and the stability margin ([13], p. 141). Fig. 10 shows a graphical representation of the absolute sensitivity. The black line in Fig. 10 denotes the absolute sensitivity associated with the fractional controller of the paper, the red and blue line denotes absolute sensitivity associated with Monje et al. [21] and Bettayeb and Mansouri [6] respectively. The maximum absolute sensitivity $S_{\max}$ is a good measure of the robustness. The maximum absolute sensitivity is the reciprocal of the stability margin [4]. The maximum absolute sensitivity $S_{\max}$ of the proposed closed-loop is 1.33, see Fig. 10. That is an improvement by 3.7% from the maximum sensitivity of Monje et al. [21] closed-loop and by 8% from that of the Bettayeb and Mansouri [6] closed-loop.

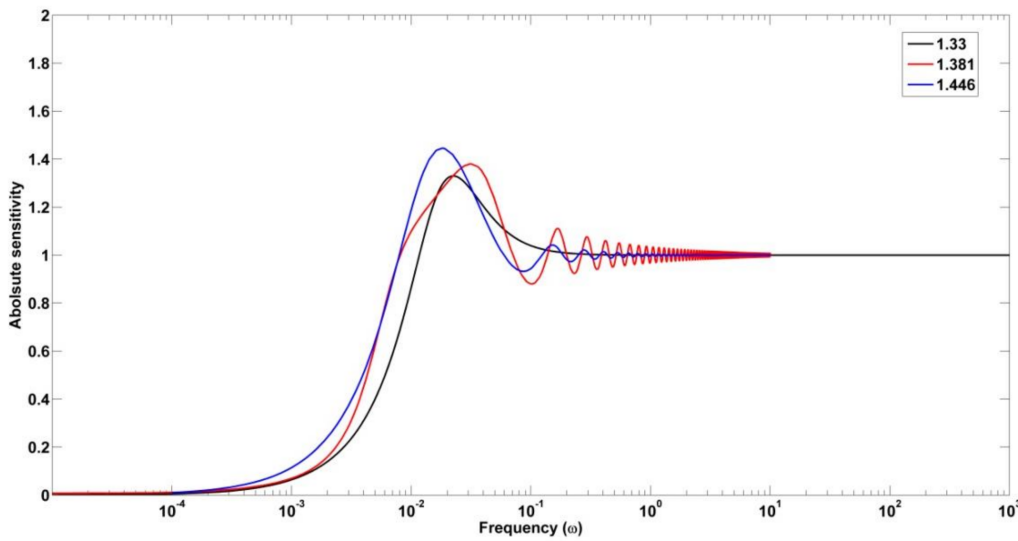

Figure 10: A graphical representation of the absolute sensitivity for liquid level system

The relatively less value of $S_{\max}$, associated with the proposed controller, suggests the less amplification of the disturbances occurring at frequencies such that $|g(j\omega)| > 1$, where $|g(j\omega)|$ is the absolute sensitivity ([4], p. 323). The less value of $S_{\max}$ for the proposed controller also confirms greater stability margin of the proposed closed-loop.

4.2. MIMO example

After a successful demonstration of the proposed fractional controller on single-input, single-output example, consider second example of a 'Shell control fractionator problem' listed by the company in the First Shell Process Control workshop [29, 36]. This Shell control problem, available in Ogunnaike and Ray [24], is considered to be a benchmark problem for providing a standard and realistic test bed for assessment of fresh control theories and technologies.

Here, we revisit the Shell control fractionator with two outputs and three inputs. The problem received attention in the literature [11, 30]. The transfer matrix representing the dynamic behaviour of the mentioned problem is given as

$$G_p(s) = \begin{pmatrix} \dfrac{4.05\,e^{-81s}}{50s+1} & \dfrac{1.77\,e^{-89s}}{60s+1} & \dfrac{5.88\,e^{-81s}}{50s+1} \\ \dfrac{5.39\,e^{-54s}}{50s+1} & \dfrac{5.72\,e^{-42s}}{60s+1} & \dfrac{6.9\,e^{-45s}}{40s+1} \end{pmatrix}. \tag{22}$$

Now as there are unequal number of inputs and outputs in the system matrix, the proper controller pairing becomes imperative. The controller pairing allows the decentralized control of MIMO processes [33]. Since the fractionator problem has a non-square matrix description, we utilize the non-square RGA mentioned in Section 2.2. The steady state gain matrix $G_p(0)$ is obtained by evaluating the transfer matrix $G_p(s)$ at $s = 0$. After using (1) and (22), the non-square fractionator RGA matrix λ^N can be found as

$$\lambda^N = \begin{pmatrix} 0.3203 & -0.5946 & 1.2744 \\ -0.017 & 1.5733 & -0.5563 \end{pmatrix}. \tag{23a}$$

The matrix λ^N of (23a) suggests the $(y_1 - u_3/y_2 - u_2)$ pairing for the decentralized control configuration, since $\lambda_{13} > 0.5$, $\lambda_{22} > 0.5$. Alternatively, the non-square fractionator RNGA matrix λ^{RN} resulting from (2) and (22) is found as

$$\lambda^{RN} = \begin{pmatrix} 0.6492 & -0.5916 & 0.9424 \\ -0.3018 & 1.5825 & -0.2807 \end{pmatrix}. \tag{23b}$$

On observing the non-square fractionator RNGA of (23b), it can be confirmed that (23b) also suggests the $(y_1 - u_3/y_2 - u_2)$ pairing. Now, the next step is to design two controller transfer functions. The first controller output is the third fractionator input and the second controller output becomes the second fractionator input. Thus, the fractionator controller transfer functions based on the same procedure as adopted in example 4.1 are given by

$$G_{c_1}(s) = \frac{1}{88.2\,s^{0.0205} - 81}\left(15.391 + \frac{0.17}{s} + 344.39\,s\right), \tag{24}$$

$$G_{c_2}(s) = \frac{1}{48.56\, s^{0.015} - 42}\left(14.16 + \frac{0.1748}{s} + 220.28\, s\right). \tag{25}$$

Here, the filter fractionality $\gamma = 0.0205$ and $\gamma = 0.015$ corresponds to overshoot 0.013 and 0.003 for the controlled output Y_1 and Y_2 respectively. Note that, the decentralized control method adopted in this paper is applicable for multi-input, multi-output (MIMO) systems with moderate time delay. For larger time delay MIMO systems, interactions strengthen out. In such scenarios dedicated multivariable decoupling control strategy may be employed in addition to the proposed method to deal with such systems [33, p. 477].

Similar to the SISO example the stability analysis of the fractionator example also hinges to the Riemann surface. The structure of the fractional characteristic polynomial associated with the *fractionator* closed-loop setup for both inputs-outputs would be the same, see (21). The specific structure of the fractional characteristic polynomial associated with the closed-loop of both the outputs Y_1 and Y_2 are

$$f_1(s) = 88.2s^{1.0205} - 40.5s + 1, \qquad f_2(s) = 48.56s^{1.015} - 22s + 1,$$

respectively. Choosing $\lambda = s^{\beta}$, the associated characteristic polynomials becomes

$$\begin{aligned} f_1(\lambda^{1/\beta}) &= \widetilde{f_1}(\lambda) = 88.2\lambda^{2041} - 40.5\lambda^{2000} + 1, \\ f_2(\lambda^{1/\beta}) &= \widetilde{f_2}(\lambda) = 48.5\lambda^{203} - 22\lambda^{200} + 1, \end{aligned} \tag{26}$$

where $s^{0.0005} = \lambda$ and $s^{0.005} = \lambda$ for the first and second polynomials respectively. Fig. 11(a) and Fig. 11(b) display the stability assessment for two closed-loop systems associated with the controlled outputs Y_1 and Y_2 respectively. The associated characteristic polynomials of (26) are displayed on the Riemann surface, see Fig. 11.

It is observed from Fig. 11 that no angles of roots of the associated characteristic polynomials for both the closed-loops associated with the outputs Y_1 and Y_2 lie inside the principal sheet of the Riemann surface. That is suggestive of the stable closed-loop system. The graphical analysis in Fig. 11 confirms the stability of the fractional system of MIMO example, i.e. the condition $|\angle\lambda_i| > \dfrac{\beta\pi}{2}$ holds for the associated characteristic polynomial.

To show the superiority of the designed fractionator controllers of this paper, a unit step setpoint change in the reference Y_{r1} of the output Y_1 is given. Note that the second output Y_2 is setpoint change-free. The results of this step change, which influence both the closed-loop fractionator outputs, are compared with the multivariable PI controlled fractionator outputs of Rao and Chidambaram [30] and Chen et al. [11], see Fig. 12. Here, to evaluate the performance of three pairs

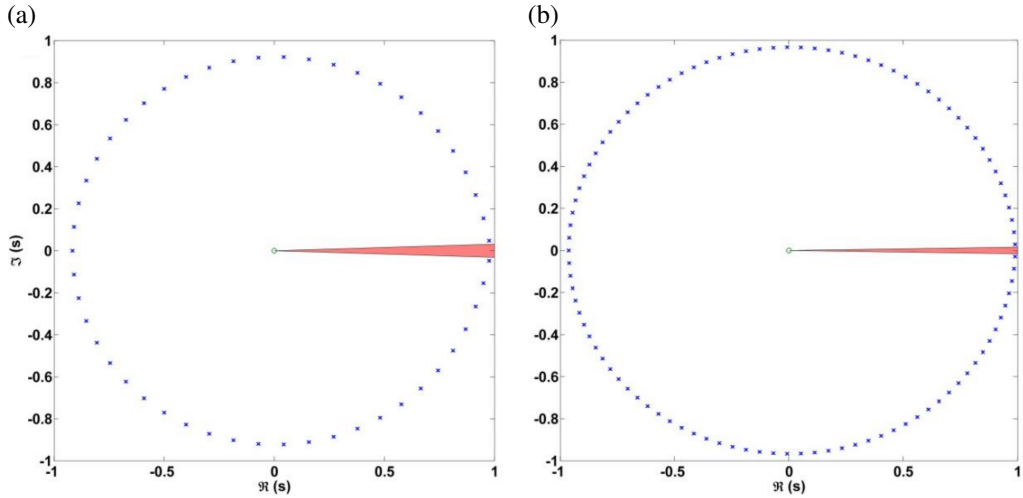

Figure 11: Stability assessment for closed-loop systems of MIMO fractionator example

of controllers, Integral Absolute Error (IAE) and Integral Square Control Input (ISCI) performance criteria are adopted.

Figs. 12(a) and 12(b) show the efficacy of the controllers G_{c_1} and G_{c_2} of this paper in the sense that the IAE and ISCI [39] resulting from the proposed method

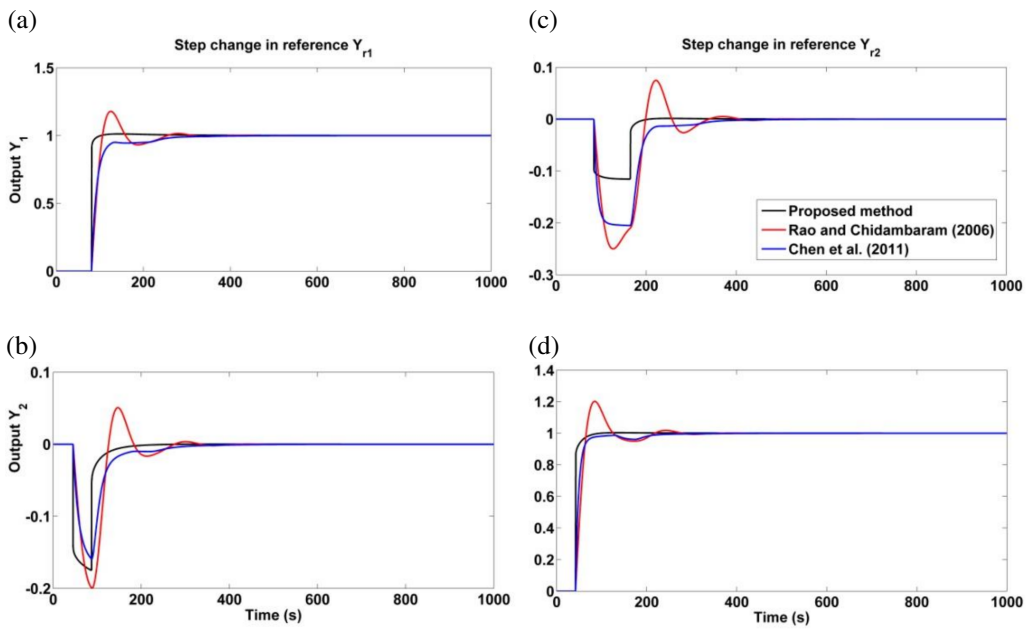

Figure 12: Closed-loop step response with a unit step change in Y_{r1} and Y_{r2}

are less than that of the IAE and ISCI resulting from the other two methods. It is clear from the representation in Fig. 12 that the proposed controller achieves quicker settling of the response with a reduced overshoot. This achievement is attributed to the combined effect of the fractional filter and the Smith predictor adopted in this paper. Fig. 12(b) shows the response of controlled output Y_2 for interactions from the first loop. The peak is higher for the proposed method in contrast to Chen et al. [11] and lesser in comparison to Rao and Chidambaram [30]. However, on the contrary, the settling is quite faster for the proposed method in comparison to the other methods.

Now, we consider a unit step setpoint change Y_{r2} of the second output Y_2 and the first output is setpoint change-free. It can be observed from Fig. 12(c) that the interactions occurring in the controlled output Y_1 have quite less overshoot and even faster settling resulting from the proposed method in contrast to the other available methods. The same revelations are achieved about the IAE and ISCI values, see Figs. 12(c) and 12(d).

In addition to graphical illustrations, the IAE and ISCI values of the fractionator controlled outputs using three methods are listed in Table 2. The first part of Table 2 discusses the IAE performance indices and the second part is about the control efforts indices (ISCI).

Table 2: Performance indices of the fractionator controlled outputs

		The IAE for fractionator outputs			Control effort in the inputs (ISCI)		
		Proposed method	Rao and Chidambaram [30]	Chen et al. [11]	Proposed method	Rao and Chidambaram [30]	Chen et al. [11]
Step change in Y_{r1}	$Y_1 - Y_{r1}$	3.063	18.78	16.59	33.47	35.72	34.62
	$Y_2 - Y_{r1}$	0.4172	3.541	1.905	1.195	1.3	1.19
Step change in Y_{r2}	$Y_1 - Y_{r2}$	0.3447	4.809	3.45	0.419	1.434	1.314
	$Y_2 - Y_{r2}$	2.414	19.12	10.07	37.9	41.65	40.1

For example, the ISCI value for the step change in Y_{r1} associated with the proposed controller is 33.47 compared to 35.72 and 34.62 for the Rao and Chidambaram [30] and Chen et al. [11] method respectively, see Table 2. A similar interpretation can be made for the ISCI values for the step change in Y_{r2}. The IAE and ISCI values of Table 2 are indicative of the effective improvement in the performance of the proposed method compared to the methods available in literature.

Fig. 13 shows the disturbance rejection response of the proposed method as compared to that of the appealing methods available in the literature [11, 30]. Fig. 13(a) and Fig. 13(c) display the disturbance rejection response for the outputs Y_1 and Y_2 respectively. Fig. 13(b) and Fig. 13(d) display the control effort graphs

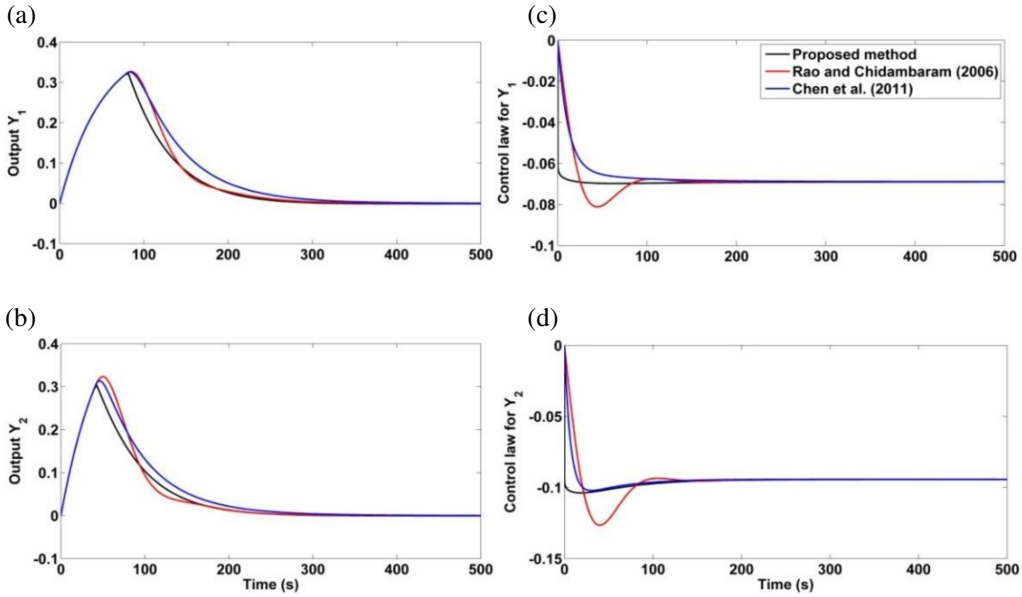

Figure 13: Disturbance rejection response for outputs Y_1 and Y_2

associated with the controlled outputs Y_1 and Y_2 respectively. The disturbance transfer functions for both controlled outputs Y_1 and Y_2 are

$$\frac{Y_1(s)}{D_1(s)} = \frac{357.21s^{1.0205} - 328.05}{(88.2s^{1.0205} - 40.5s + 1)(50s + 1)} e^{-81s}, \tag{27}$$

$$\frac{Y_2(s)}{D_2(s)} = \frac{261.74s^{1.015} - 226.38}{(48.56s^{1.015} - 21s + 1)(50s + 1)} e^{-54s}. \tag{28}$$

respectively. Numerical simulations demonstrated in Fig. 13 are the consequence of a set of two disturbance transfer functions, see (27) and (28). Note that $D_1(s)$ and $D_2(s)$ are the Laplace transforms of the disturbance input signals associated with the outputs Y_1 and Y_2 respectively. Fig. 13 reveals the following: (i) relatively less value of the overshoot arising from the proposed method in contrast to the other two methods. (ii) The control effort graphs show quick settling of the control actions for the proposed method indicating fewer efforts put by the proposed controller in lieu of the other methods available in the literature, see Fig. 13(c) and Fig. 13(d). The disturbance rejection response clearly explains the relatively enhanced response of the proposed controller.

Here, we analyze the disturbance rejection responses using IAE values for the nominal and mismatch cases. The IAE values for the disturbance rejection response associated with the controlled fractionator resulting from the three

methods are listed in Table 3. Table 3 also depicts the IAE values for the 5% mismatch case as well.

Table 3: IAE values for disturbance rejection response

Method	Output Y_1		Output Y_2	
	Nominal case	5% mismatch case	Nominal case	5% mismatch case
Proposed method	0.8797	0.9102	0.9576	0.9717
Rao and Chidambaram [30]	2.645	2.76	3.36	3.432
Chen et al. [11]	6.447	6.78	5.204	5.474

For example, the IAE values for the disturbance rejection associated with the output Y_1 are 0.8797 and 0.9102 for the nominal and mismatch cases respectively. That are relatively less than the IAE values of the other two methods, see Table 3. A similar interpretation for the output Y_2 can be made. The IAE values in Table 3 are indicative of better performance resulting from the proposed method compared to the available methods in the literature under two cases, i.e. the nominal and mismatch cases.

Fig. 14 displays the graphical representation of the sensitivity functions for three control methods. Here the sensitivity function associated with the proposed method is compared to that of the other two methods [11, 30]. Fig. 14(a) and Fig. 14(b) show the sensitivity plots for the outputs Y_1 and Y_2 respectively. Table 4 lists the maximum absolute sensitivity for the closed-loop system associated with

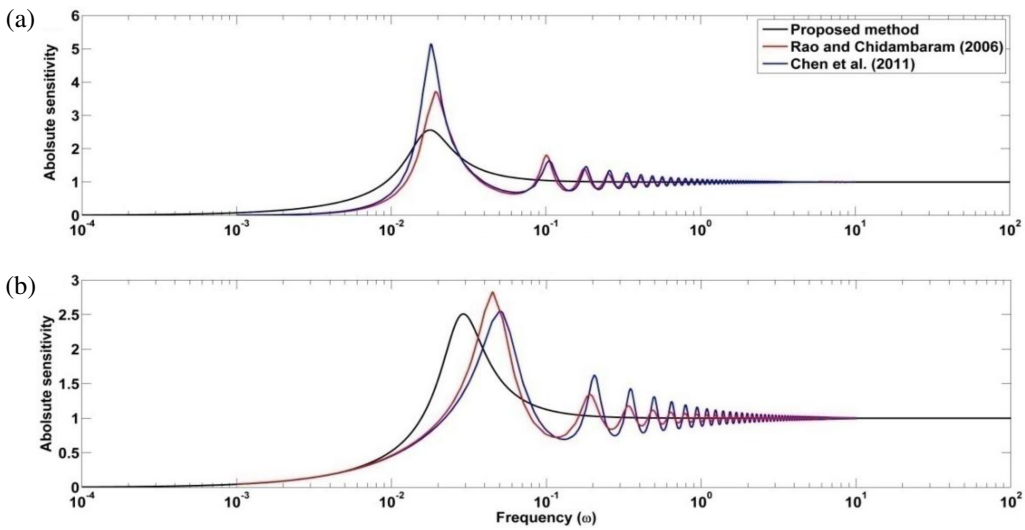

Figure 14: A graphical representation of the absolute sensitivity for both the control loops

both the outputs. The $S_{\max}$ values in Table 4 reveal that there is a substantial improvement in the absolute maximum sensitivity measure associated with the proposed method. This confirms a notable improvement in the stability margin of the closed-loop resulting from the proposed controller. Hence, the proposed method shows a notable performance for the multi-input multi-output system as well.

Table 4: Robustness performance index

	$S_{\max}$		
	Proposed method	Rao and Chidambaram [30]	Chen et al. [11]
Output Y_1	2.56	3.72	5.15
Output Y_2	2.5	2.83	2.557

5. Conclusion

This paper develops a generalized theory of the fractional order controller transfer function for integer order time-delay systems. That can be regarded as an extension of the fractional control to a dead time compensator problem. Then, generalized fractional-filter PID order controller transfer functions for several other systems with dead time were achieved, illustrated in Table A. Investigations for the combined effect of the fractional filter and the Smith predictor in the feedback setup are carried out. This paper reveals how the combination of Smith predictor and fractional filter contributes to restrict the overshoot and improving the overall response. We have demonstrated the ability of the generalized fractional control of this paper using the disturbance rejection, robustness analysis, IAE as well as ISCI indices. Investigations carried out on the developed fractional controller of the paper reveals enhanced closed-loop results. The paper also discusses the stability of the proposed closed-loop using the notion of fractional characteristics polynomial. Thus, the universality of the findings of the paper will be useful to attempt practical control problems that possess time delays.

Appendix A

Here, we list the fractional filter transfer function that accounts for the Smith predictor correction term and the PID controller parameters for the several other time-delay systems. That is a consequence of the Theorem of the paper. The paper abandons the claim for the completeness of the controller transfer function table. A similar procedure can be adopted to achieve the generalized fractional-filter PID controller for n-th order time-delay systems.

Table A: PID parameters and fractional filter transfer functions for dead time processes

Sr. No.	$G_p(s)$	Fractional filter	k_p	k_i	k_d
1.	$\frac{ke^{-t_d s}}{\tau s+1}$	$\frac{1}{\tau_c s^\gamma - \frac{t_d}{2}}$	$\frac{\tau+\frac{t_d}{2}}{k}$	$\frac{1}{k}$	$\frac{\tau t_d}{2k}$
2.	$\frac{ke^{-t_d s}}{(\tau_1 s+1)(\tau_2 s+1)}$	$\frac{1+\frac{t_d s}{2}}{\tau_c s^\gamma - \frac{t_d}{2}}$	$\frac{\tau_1+\tau_2}{k}$	$\frac{1}{k}$	$\frac{\tau_1 \tau_2}{k}$
3.	$\frac{k(\tau_3 s+1)e^{-t_d s}}{(\tau_1 s+1)(\tau_2 s+1)}$	$\frac{1+\frac{t_d s}{2}}{(\tau_3 s+1)(\tau_c s^\gamma - t_d)}$	$\frac{\tau_1+\tau_2}{k}$	$\frac{1}{k}$	$\frac{\tau_1 \tau_2}{k}$
4.	$\frac{ke^{-t_d s}}{s}$	$\frac{1}{\tau_c s^\gamma - \frac{t_d}{2}}$	$\frac{1}{k}$	–	$\frac{t_d}{2k}$
5.	$\frac{ke^{-t_d s}}{s(\tau s+1)}$	$\frac{1+\frac{t_d s}{2}}{\tau_c s^\gamma - \frac{t_d}{2}}$	$\frac{1}{k}$	–	$\frac{\tau}{k}$
6.	$\frac{ke^{-t_d s}}{T^2 s^2+2\xi T s+1}$	$\frac{1+\frac{t_d s}{2}}{\tau_c s^\gamma - \frac{t_d}{2}}$	$\frac{2\xi T}{k}$	$\frac{1}{k}$	$\frac{T^2}{k}$
7.	$\frac{k(1-Bs)e^{-t_d s}}{\tau s+1}$	$\frac{1}{\tau_c s^\gamma + \frac{Bt_d s}{2} + B - \frac{t_d}{2}}$	$\frac{\tau+\frac{t_d}{2}}{k}$	$\frac{1}{k}$	$\frac{\tau t_d}{2k}$
8.	$\frac{k(1-Bs)e^{-t_d s}}{T^2 s^2+2\xi T s+1}$	$\frac{1+\frac{t_d s}{2}}{\tau_c s^\gamma + \frac{Bt_d s}{2} + B - \frac{t_d}{2}}$	$\frac{2\xi T}{k}$	$\frac{1}{k}$	$\frac{T^2}{k}$
9.	$\frac{k(1-Bs)e^{-t_d s}}{s(\tau s+1)}$	$\frac{1+\frac{t_d s}{2}}{\tau_c s^\gamma + \frac{Bt_d s}{2} + B - \frac{t_d}{2}}$	$\frac{1}{k}$	–	$\frac{\tau}{k}$

Appendix B

The proposed controller embeds a fractional filter cascaded with a PID controller for the specific plant setup. The PID controller implementation is straight-

forward. However, the fractional filter can be implemented using the notion of equivalent systems. In practice, considering a band limit with a proper range of frequencies, implementation of the fractional order filter can be achieved ([41], p. 58). Here, we explain a method, an equivalent integer-order Oustaloup filter transfer function $F_f(s)$ to a fractional filter with the fractionality γ, which can be designed as

$$F_f(s) = K \prod_{1 \leqslant \kappa \leqslant N} \frac{s + \psi'_\kappa}{s + \psi_\kappa},$$

where $\psi'_\kappa = \psi_l \psi_a^{(2\kappa - 1 - \gamma)/N}$, $\psi_\kappa = \psi_l \psi_a^{(2\kappa - 1 + \gamma)/N}$, $K = \psi_h^\gamma$ with $\psi_a = \sqrt{\dfrac{\psi_h}{\psi_l}}$.

Here, N is the order of the integer filter, ψ_h and ψ_l are the upper and the lower operating frequencies. To demonstrate the method, we explain the procedure to get the integer order filter. Suppose $N = 2$, $\gamma = 0.5$ with 1000 rad/s and 0.01 rad/s as the upper ψ_h and the lower ψ_l frequency band limit respectively. Then, the Oustaloup filter transfer function becomes

$$F_f(s) = \frac{31.62s^2 + 423.7s + 17.7}{s^2 + 237.9s + 177.86}.$$

For the brevity of presentations, we have demonstrated a simple case. The detail can be found in [25, 41].

References

[1] G. Alevisakis and D.E. Seborg: An extension of the smith predictor method to multivariable linear systems containing time delays, *International Journal of Control*, **17**(3) (1973), 541–551, doi: 10.1080/00207177308932401.

[2] K. Amoura, R. Mansouri, M. Bettayeb, and U.M. Al-Saggaf: Closed-loop step response for tuning PID-fractional-order-filter controllers, *ISA Transactions*, **64** (2016), 247–257.

[3] K.J. Åström and T. Hägglund: *PID controllers: Theory, design, and tuning*, Research Triangle Park, NC: Instrument Society of America, 1995.

[4] K.J. Åström and R.M. Murray: *Feedback Systems: An Introduction for Scientists and Engineers*, New Jersey, Princeton University Press, 2008.

[5] R.S. Barbosa, J.A.T Machado, and I.M. Ferreira: Tuning of PID Controllers Based on Bode's Ideal Transfer Function, *Nonlinear Dynamics*, **38** (2004), 305–321, doi: 10.1007/s11071-004-3763-7.

[6] M. Bettayeb and R. Mansouri: IMC-PID-fractional-order-filter controllers design for integer order systems, *ISA Transactions*, **53**(5) (2014), 1620–1628.

[7] K. Bingi, R. Ibhrahim, M.N. Karsiti, S.M. Hassan, and V.R. Harindran: A comparative study of 2DOF PID and 2DOF fractional order PID controllers on a class of unstable systems, *Archives of Control Sciences*, **28**(4) (2018), 635–682.

[8] H.W. Bode: *Network Analysis and Feedback Amplifier Design*, New York, Van Nostrand, 1945.

[9] E.H. Bristol: On a new measure of interaction for multivariable process control, *IEEE Transactions on Automatic Control*, **11**(1) (1966), 133–134, doi: 10.1109/TAC.1966.1098266.

[10] J.W. Chang and C.C. Yu: The relative gain for non-square multivariable systems, *Chemical Engineering Science*, **45**(5) (1990), 1309–1323, doi: 10.1016/0009-2509(90)87123-A.

[11] J. Chen, Z.F. He and X. Qi: A new control method for MIMO first order time delay non- square systems, *Journal of Process Control*, **21**(4) (2011), 538–546, doi: 10.1016/j.jprocont.2011.01.007.

[12] C.E. Garcia and M. Morari: Internal model control. A unifying review and some new results, *Industrial & Engineering Chemistry Process Design and Development*, **21** (1982), 308–321.

[13] G.C. Goodwin, S.F. Graebe, and M.E. Salgado: *Control Systems Design*, Prentice Hall, 2001.

[14] F.A. Graybill, C.D. Meyer, and R.J. Painter: Note on the generalized inverse of the product of matrices, *SIAM Reviews*, **8**(4) (1966), 522–524.

[15] C-C. Hantschk: Pressure pulsations in industrial combustion systems due to self-excitation, in *Proc. 4th International conference on Structural Dynamics*, EURODYN (2002), 387–391.

[16] M.J. He, W.J. Cai, W. Ni, and L.H. Xie: RNGA based control system configuration for multivariable processes, textitJournal of Process Control, **19**(6) (2009), 1036–1042, doi: 10.1016/j.jprocont.2009.01.004.

[17] T. Kaczorek: *Selected Problems of Fractional Systems Theory*, LNCIS, Berlin, Springer-Verlag, 2011.

[18] MathWorks: *Curve Fitting Toolbox For Use with MATLAB*, Version 1.1.2, The MathWorks, Inc., 2004.

[19] M. Minorsky: Self-excited oscillations in dynamical systems possessing retarded actions, *Journal of Applied Mechanics*, **9** (1942), 465.

[20] C.A. Monje, Y.Q. Chen, B.M. Vinagre, D. Xue, and V. Feliu: *Fractional-order Systems and Controls: Fundamentals and Applications*, London, Springer-Verlag, 2010.

[21] C.A. Monje, B.M. Vinagre, V. Feliu, and Y.Q. Chen: Tuning and auto-tuning of fractional order controllers for industry applications, *Control Engineering Practice*, **16**(7) (2008), 798–812.

[22] C.F. Moore, C.L. Smith, and P.W. Murrill: Improved algorithm for direct digital control, *Instuments and Control Systems*, **43** (1970), 70.

[23] M. Morari and E. Zafiriou: *Robust Process Control*, Englewood Cliffs, Prentice Hall, 1991.

[24] B.A. Ogunnaike and W.H. Ray: *Process Dynamics, Modeling and Control*, Oxford University Press, New York, 1994.

[25] K. Oprzedkiewicz: Approximation method for a fractional order transfer function with zero and pole, *Archives of Control Sciences*, **24**(4) (2014), 447–463.

[26] A. Oustaloup, F. Levron, B. Mathieu, and F.M. Nanot: Frequency-band complex noninteger differentiator: Characterization and synthesis, *IEEE Transactions on Circuits and Systems I: Fundamental Theory and Applications*, **47**(1) (2000), 25–39, doi: 10.1109/81.817385.

[27] N.S. Özbek, M. Önkol, and M.Ö. Efe: Feedback control strategies for quadrotor-type aerial robots: A survey, *Transactions of Institute of Measurement and Control*, **38**(5) (2015), 529–554, doi: 10.1177/0142331215608427.

[28] I. Podlubny: Fractional-order systems and $PI^{\lambda}D^{\mu}$ controllers, *IEEE Transactions on Automatic Control*, **44**(1) (1999), 208–214, doi: 10.1109/9.739144.

[29] D.M. Prett and M. Morari: *The Shell process control workshop*, London, Butterworths, 1987.

[30] A.S. Rao and M. Chidambaram: Smith delay compensator for multivariable non-square systems with multiple time delays, *Computers & Chemical Engineering*, **30**(8) (2006), 1243–1255, doi: 10.1016/j.compchemeng.2006.02.017.

[31] D.E. Rivera, M. Morari, and S. Skogestad: Internal model control. 4. PID controller design, *Industrial & Engineering Chemistry Process Design and Development*, **25** (1986), 252–265.

[32] D.E. Reeves and Y. Arkun: Interaction measures for nonsquare decentralized control structures, *AIChE Journal.*, **35**(45) (1989), 603–613, doi: 10.1002/aic.690350410.

[33] D.E. Seborg, T.F. Edgar, and D.A. Mellichamp: *Process Dynamics and Control*, John Wiley and sons, New York, 2004.

[34] O.J.M. Smith: Closer control of loops with dead time, *Chemical Engineering Progress*, **53** (1957), 217–219.

[35] G. Stephanopoulos: *Chemical Process Control*, Englewood Cliffs, New Jersey, Prentice Hall, 1984.

[36] C. Vlachos, D. Williams, and J.B. Gomm: Solution to the shell standard control problem using genetically tuned PID controllers, *Control Engineering Practice*, **10**(2) (2002), 151–163, doi: 10.1016/S0967-0661(01)00115-0.

[37] Q.G. Wang, B. Huang, and X. Guo: Auto-tuning of TITO decoupling controllers from step tests, *ISA Transactions*, **39** (2000), 407–418, doi: 10.1016/S0019-0578(00)00028-8.

[38] Q.G. Wang, B. Zou, T.H. Lee, and Q. Bi: Auto-tuning of multivariable PID controllers from decentralized relay feedback, *Automatica*, **33**(3) (1997), 319–330, doi: 10.1016/S0005-1098(96)00177-X.

[39] S.K.P. Wong and D.E. Seborg: A theoretical analysis of Smith and analytical predictors, *AIChE Journal*, **32**(10) (1986), 1597–1605, doi: 10.1002/aic.690321003.

[40] E. Yumuk, M. Güzelkaya, and I. Eksin (in press): Analytical fractional PID controller design based on Bode's ideal transfer function plus time delay, *ISA Transactions* (2019), doi: 10.1016@j.isatra.2019.01.034.